

Article

Assessing the Urban Eco-Environmental Quality by the Remote-Sensing Ecological Index: Application to Tianjin, North China

Ting Zhang ^{1,†}, Ruiqing Yang ^{2,*}, Yibo Yang ³, Long Li ^{1,4}  and Longqian Chen ¹

¹ School of Public Policy and Management, China University of Mining and Technology, Daxue Road 1, Xuzhou 221116, China; tingzhang@cumt.edu.cn (T.Z.); long.li@vub.be (L.L.); chenlq@cumt.edu.cn (L.C.)

² College of Resources and Environment, Huazhong Agricultural University, Shizishan Street 1, Wuhan 430070, China

³ School of Public Administration, China University of Geosciences, Lumo Road 388, Wuhan 430074, China; yibo.yang@cug.edu.cn

⁴ Department of Geography & Earth System Science, Vrije Universiteit Brussel, 1050 Brussels, Belgium

* Correspondence: ruiqing.yang@webmail.hzau.edu.cn; Tel.: +86-158-2705-2818

† These authors contributed equally to this work and should be considered as co-first authors.

Abstract: The remote-sensing ecological index (RSEI), which is built with greenness, moisture, dryness, and heat, has become increasingly recognized for its use in urban eco-environment quality assessment. To improve the reliability of such assessment, we propose a new RSEI-based urban eco-environment quality assessment method where the impact of RSEI indicators on the eco-environment quality and the seasonal change of RSEI are examined and considered. The northern Chinese municipal city of Tianjin was selected as a case study to test the proposed method. Landsat images acquired in spring, summer, autumn, and winter were obtained and processed for three different years (1992, 2005, and 2018) for a multitemporal analysis. Results from the case study show that both the contributions of RSEI indicators to eco-environment quality and RSEI values vary with the season and that such seasonal variability should be considered by normalizing indicator measures differently and using more representative remote-sensing images, respectively. The assessed eco-environment quality of Tianjin was, overall, improving owing to governmental environmental protection measures, but the damage caused by rapid urban expansion and sea reclamation in the Binhai New Area still needs to be noted. It is concluded that our proposed urban eco-environment quality assessment method is viable and can provide a reliable assessment result that helps gain a more accurate understanding of the evolution of the urban eco-environment quality over seasons and years.

Keywords: urban eco-environment quality; remote sensing ecological index; seasonal variability



Citation: Zhang, T.; Yang, R.; Yang, Y.; Li, L.; Chen, L. Assessing the Urban Eco-Environmental Quality by the Remote-Sensing Ecological Index: Application to Tianjin, North China. *ISPRS Int. J. Geo-Inf.* **2021**, *10*, 475. <https://doi.org/10.3390/ijgi10070475>

Academic Editors: Niko Lukač, Marko Bizjak and Wolfgang Kainz

Received: 18 May 2021

Accepted: 9 July 2021

Published: 10 July 2021

Publisher's Note: MDPI stays neutral with regard to jurisdictional claims in published maps and institutional affiliations.



Copyright: © 2021 by the authors. Licensee MDPI, Basel, Switzerland. This article is an open access article distributed under the terms and conditions of the Creative Commons Attribution (CC BY) license (<https://creativecommons.org/licenses/by/4.0/>).

1. Introduction

The eco-environment is defined as “the total quantity and quality of water resources, land resources, biological resources and climate resources that affect human survival and development.” [1]. It is a social-economic-natural compound system and an essential element for human subsistence [1]. Unlike the environment, which only contains non-biological factors, the eco-environment is a holistic system with complex ecological relationships [2]. Nowadays, urban eco-environment quality plays an increasingly important role in urban eco-environmental processes, climatic change, land use, and human health [1–3]. While rapid urbanization accompanies economic prosperity, its negative effects that threaten sustainable urban development cannot be ignored ranging from land degradation to climate warming [4]. How to scientifically determine the state of urban eco-environment quality as well as provide a quantitative analysis is among top priorities and has been receiving increased attention.

Traditionally, semi-quantitative methods such as the analytical hierarchy process (AHP) and the weighted linear combination (WLC) are used for eco-environment quality assessment [5,6]. They are considered subjective and less applicable when many indicators are required [7]. These limitations can, however, be to some extent overcome by remote sensing. With its capability of imaging large areas in a repeated manner, remote sensing has now been widely applied to a variety of urban eco-environment quality studies and applications including urban eco-environment quality assessment. Many indicators required in the assessment can be directly or indirectly derived from remote-sensing image data at different sensor resolutions over a long period, allowing the assessment to be conducted on various spatial and temporal scales [8]. For this reason, over the past two decades, remote sensing has often been combined with various assessment methods [9,10].

Some studies used remote sensing to obtain a single eco-environmental assessment factor, such as a vegetation index or land surface temperature, for assessing the urban eco-environment quality in areas like forests, wetlands, and cities [11–13]. But a single eco-environmental assessment factor is insufficient for characterizing complex urban eco-environmental quality and fails to consider the contribution of many other eco-environmental assessment factors to an ecosystem. In response to those challenges, Xu et al. proposed a remote-sensing ecological index (RSEI) with four indicators representing greenness, humidity, heat, and dryness respectively and tested it to Xiong'an New Area, Fuzhou, and many other areas in China [14–16]. They found that urban expansion is responsible largely for increasing impervious surfaces and deteriorating surface urban eco-environmental quality [17]. In comparison with the original ecological index in China's Technical Criterion for Ecosystem Status Evaluation (Trial) (HJ192–2015), the RSEI is considered easier for application and more convenient for updates in the need of monitoring a changing urban eco-environment quality [18].

In recent years, the RSEI has grown in popularity and been frequently adopted for urban eco-environment quality assessment in individual cities such as Pingtan Comprehensive Pilot Zone [19] in China, regions such as the Beijing–Tianjin–Hebei region [20], the Guangdong–Hong Kong–Macau Bay area [21], the Chaohu basin [22,23], and the Beijing–Hangzhou Canal coast [24], and even at a national scale [25]. It has also been applied by international researchers, for example, to Gaomishan City in Iran [26], the Samara region of Russia [27], as well as different cities in the United States [28] and Europe [29]. These studies usually calculated annual RSEI from individual remote-sensing images and then performed a multi-year analysis of the change in eco-environmental conditions [30]. Because eco-environmental conditions in a given area do not necessarily remain the same throughout a year, there is a need to consider the seasonal and even monthly variability of RSEI if remote-sensing image data become available. In addition, the principal component analysis (PCA) method is a multi-dimensional data compression technology that can remove any impact of co-linearity between the four variables [31], and these studies rarely examined the nature of the contribution of the indicators to the eco-environment quality before the implementation of principal component analysis, and the RSEI model might be inappropriately constructed for not correcting the direction of eigenvectors [22].

In this study, therefore, we propose a new urban eco-environment quality assessment method using the RSEI where seasonal variability is considered. The method was tested in Tianjin, a municipal city in North China. Landsat data acquired in spring, summer, autumn, and winter of three different years (i.e., 1992, 2005, and 2018, for the availability and quality of image data) were obtained and processed for a multi-temporal analysis. The selected years could help create a timeline for Tianjin's eco-environmental quality change at intervals of 13 years. The specific objectives of the study are as follows: (1) optimizing the normalization of the individual indicators of the RSEI model; (2) examining the seasonal variability of RSEI and its impact on the assessment; and (3) characterizing the spatiotemporal change of Tianjin's urban eco-environment quality over the 26 years.

2. Study Area

As one of China’s four municipalities, Tianjin (38°34′–40°15′ W, 116°43′–118°04′ E) covers a geographical area of 11,916.85 km², located in North China on the shore of the Bohai Sea and bordered by Hebei province and Beijing to the north, west, and south (Figure 1a). Tianjin is generally flat with an average altitude of 3.3 m but hilly in the far north—its highest point is Jiuding Peak in the district of Jizhou, at an altitude of 1078.5 m. Due to its situation between the mid-latitude coastal and inland transition zone, Tianjin has a typical warm temperate semi-humid continental monsoon climate with an average annual maximum temperature of 18.6 °C, an average annual minimum temperature of 9.7 °C, and average annual precipitation of 43.2 mm [32]. Seasons are distinct in Tianjin with warm and rainy summers and cold and dry winters (Figure 2).

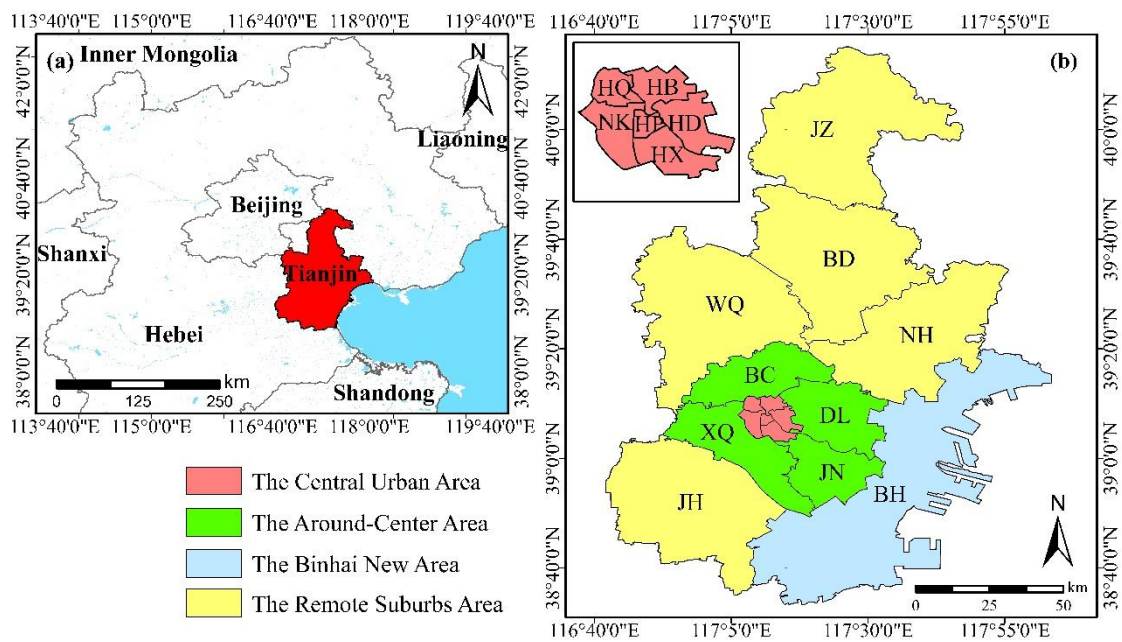


Figure 1. Study area: (a) Tianjin borders Hebei and Beijing to the norther, west, and south; (b) Tianjin consists of 16 districts which are grouped into four areas by location (full names tabulated in Table 1).

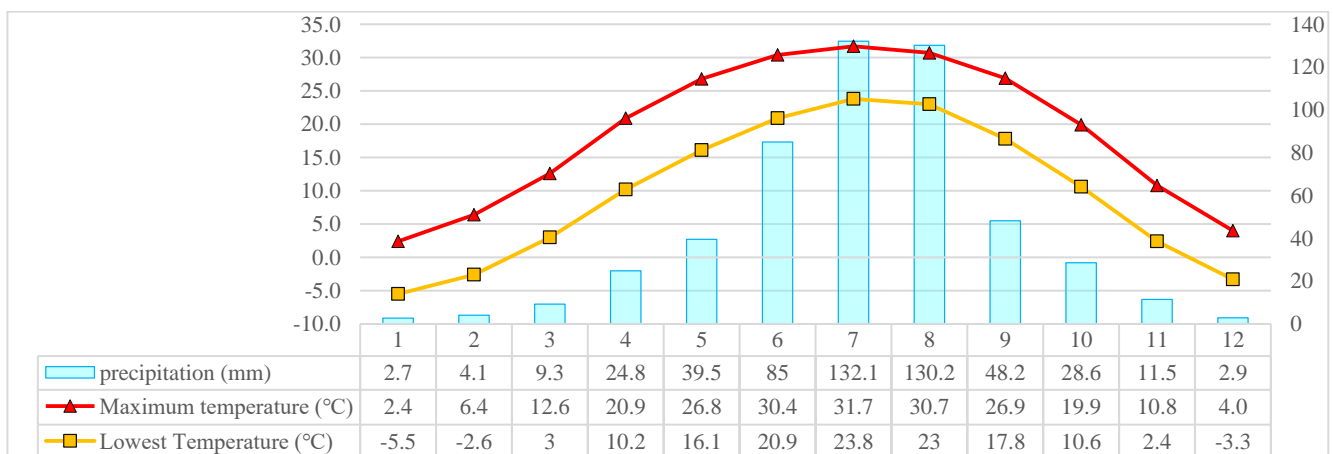


Figure 2. The weather of Tianjin in different months (1981–2010) [32].

Table 1. The districts of Tianjin.

Area	District
The Central Urban Area	Heping (HP), Hongqiao (HQ), Hebei (HB), Hexi (HX), Hedong (HD), Nankai (NK)
The Around-Center Area	Jinnan (JN), Dongli (DL), Beichen (BC), Xiqing (XQ)
The Binhai New Area	Binhaixinqu (BH)
The Remote Suburbs Area	Ninghe (NH), Jinghai (JH), Baodi (BD), Wuqing (WQ), Jizhou (JZ)

As of 2016, Tianjin has jurisdiction over 16 municipal districts, traditionally grouped into four (Figure 1b), namely the Central Urban Area, the Around-Center Area, the Binhai New Area, and the Remote Suburbs Area (Table 1). Thanks to its rapid economic development and urban expansion in recent years, Tianjin has ranked as one of China's new 15 first-tier cities from 337 Chinese cities in 2019 [33,34]. Its population increased from 9.204 million in 1992 to 15.596 million in 2018 and its economy, measured by GDP (gross domestic product) soared from 41.124 billion to 1880.964 billion RMB during the same period [35,36]. However, such socioeconomic prosperity came at the cost of tremendous consumption of resources and prominent environmental degradation. As such, the sustainable development of Tianjin was under rising pressure. The eco-environment has been reported to be generally improved [37]. Examining what Tianjin has experienced in the past three decades would help reveal the change of eco-environment in a typical Chinese city.

3. Data and Methods

3.1. Remote-Sensing Data

A total of 42 Landsat 5 and Landsat 8 satellite images for each season of 1992, 2005, and 2018 (Table 2) were collected for extracting different measures for RSEI in this study. They were acquired mostly in March for spring, in late May and early June for summer, mostly in September for autumn, and all in December for winter. It would be ideal if images were acquired on the same or very similar dates in different years, but it is not realistic because insufficient good-quality images are available for a vast region like Tianjin. Meanwhile, Landsat 7 image data were not considered in this study because they have had data gaps since May 2003 due to a technical issue. The images listed in Table 2 were the best selection that could be made at the time of the study.

Table 2. Landsat image data used in the study.

Year	Season	Path	Row	Imaging Date
1991/ 1992/ 1993	Spring	122	32/33	22 March 1991
		123	32/33	13 March 1991
	Summer	122	32/33	27 May 1992
	Autumn	122	32/33	3 September 1993
		123	32/33	25 August 1993
	Winter	122	32/33	21 December 1992
		123	32/33	28 December 1992
	2004/ 2005/ 2006	Spring	122	32/33
123			32/33	19 March 2005
Summer		122	32/33	28 May 2004
		123	32/33	19 May 2004
Autumn		122	32/33	4 September 2005
Winter		122	32/33	28 December 2006

Table 2. Cont.

Year	Season	Path	Row	Imaging Date
2018	Spring	122	32/33	16 March 2018
		123	32/33	8 April 2018
	Summer	122	32/33	4 June 2018
		123	32/33	27 June 2018
	Autumn	122	32/33	24 September 2018
		123	32/33	1 October 2018
	Winter	122	32/33	13 December 2018
		123	32/33	4 December 2018

Before extracting the measures required for constructing RSEI, these images were pre-processed for atmospheric correction (FLAASH), geo-referencing (image-to-image), and seamless mosaic, and image clipping [28,38,39]. Although different Landsat image data were used in this study, it is believed that this has a minimal effect on index calculation [38,39].

3.2. Remote-Sensing Ecological Index (RSEI) Indicators

The remote-sensing ecological index (RSEI) is a comprehensive index for rapidly detecting the eco-environmental conditions of a geographical region solely using remote-sensing data. It involves greenness, moisture, dryness, and heat, each indicating different aspects of the eco-environment, namely green vegetation, soil moisture, built-up areas and ambient temperature, respectively [14]. Each of the indicators is quantified by a measure that can be derived from remote-sensing images. Greenness, moisture, and dryness are represented by the normalized vegetation index (NDVI), the wet component of a tasseled cap transformation (wetness), and the normalized difference building-soil index (NDBSI), which is the average of the index-based built-up index (IBI) and soil index (SI) [16] respectively. Meanwhile, heat is characterized by land surface temperature (LST). Each measure is explained below.

3.2.1. Greenness—Normalized Difference Vegetation Index (NDVI)

The normalized difference vegetation index (NDVI) was proposed by Rouse et al. (1974) [40] and has become the most widely used vegetation index in remote sensing for detecting the existence and amount of green vegetation on land surfaces [41–43]. It was used by [17] here to characterize greenness in the remote sensing ecological index, given by following Equation (1):

$$NDVI = (\rho_{NIR} - \rho_{red}) / (\rho_{NIR} + \rho_{red}). \quad (1)$$

where ρ_{NIR} and ρ_{red} are the reflectance in the near-infrared (NIR) and red bands of Landsat image data, respectively.

3.2.2. Moisture—Wetness (Wet Component)

Moisture can be extracted from Landsat image data by tasseled cap transformation and represented by the resultant wet component [17]; however, the coefficients of such component vary with the sensor. The wet component (hereinafter as Wetness) was calculated for Landsat TM data using Equation (2) by Crist, Eric P. [44] and Equation (3) by Baig MHA et al. [45]. for Landsat OLI data:

$$Wet_{TM} = \rho_{blue} \times 0.0315 + \rho_{green} \times 0.2021 + \rho_{red} \times 0.3102 + \rho_{NIR} \times 0.1594 - \rho_{SWIR1} \times 0.6806 - \rho_{SWIR2} \times 0.6109 \quad (2)$$

$$Wet_{OLI} = \rho_{blue} \times 0.1511 + \rho_{green} \times 0.1973 + \rho_{red} \times 0.3283 + \rho_{NIR} \times 0.3407 - \rho_{SWIR1} \times 0.7117 - \rho_{SWIR2} \times 0.4559 \quad (3)$$

where ρ_i is the reflectance in different bands of TM and OLI data (SWIR stands for short-wave infrared).

3.2.3. Dryness—Normalized Difference Building-Soil Index (NDBSI)

The normalized difference building-soil index (NDBSI), which has been reported effective in measuring dryness [16], is computed by averaging the index-based built-up index (IBI) and soil index (SI) [46,47], each characterizing the conditions of built-up areas and bare land. The three indices are given by:

$$IBI = \frac{\frac{2\rho_{SWIR}}{\rho_{SWIR} + \rho_{NIR}} - \frac{\rho_{NIR}}{\rho_{NIR} + \rho_{Red}} - \frac{\rho_{Green}}{\rho_{Green} + \rho_{SWIR}}}{\frac{2\rho_{SWIR}}{\rho_{SWIR} + \rho_{NIR}} + \frac{\rho_{NIR}}{\rho_{NIR} + \rho_{Red}} + \frac{\rho_{Green}}{\rho_{Green} + \rho_{SWIR}}} \quad (4)$$

$$SI = \frac{(\rho_{SWIR} + \rho_{Red}) - (\rho_{NIR} + \rho_{Blue})}{(\rho_{SWIR} + \rho_{Red}) + (\rho_{NIR} + \rho_{Blue})} \quad (5)$$

$$NDBSI = \frac{IBI + SI}{2} \quad (6)$$

where ρ is the reflectance in different bands of Landsat image data.

3.2.4. Heat—Land Surface Temperature (LST)

Land surface temperature (LST), representing the heat indicator, can be estimated by the method proposed by Jiménez-Muñoz et al. [48], which has been used in many studies for deriving land surface temperature from Landsat image data [27,29]. The formula is as Equation (7):

$$T = \frac{T_B}{1 + \frac{\lambda T_B}{\rho} \ln \varepsilon} \quad (7)$$

where T is LST in K, T_B is brightness temperature in K at the sensor, λ is the effective wavelength of the thermal infrared band, ε is land surface emissivity (LSE) [49], and $\rho = 1.438 \times 10^{-2}$ mK. For the details of this method, readers are referred to Sobrino et al. [49–51] and Hu and Xu [17].

3.3. RSEI Model

3.3.1. Normalization of the Measures

Since each of the four measures was acquired in different units (e.g., LST in Celsius), it is advisable to normalize them to avoid dimensional inconsistency. In this study, the min-max normalization method [14] was adopted where all the normalized values range between 0 and 1. While Equation (8) was applied to positive contributors to the urban eco-environment quality, Equation (9) was applied to negative contributors:

$$Y_i = \frac{X_i - Min_i}{Max_i - Min_i} \quad (8)$$

$$Y_i = \frac{Max_i - X_i}{Max_i - Min_i} \quad (9)$$

where X_i and Y_i are the original and normalized values of the measures respectively and Max_i and Min_i are the maximum and minimum values of the measures, respectively. This method was used in previous studies for normalizing different measures [22,52]. As Yang et al. [53] have shown that greenness is both a positive contributor and the largest contributor to the urban eco-environment quality, the greenness measure was treated as a benchmark here and its correlation with the other measures helped to determine the nature of their contributions to the urban eco-environment quality. For this reason, a correlation analysis was conducted among the measures. Measures that are positively correlated with greenness are considered to contribute positively to urban ecological quality using

Equation (8), and measures that are negatively correlated with greenness are considered to contribute negatively to urban ecological quality using Equation (9).

3.3.2. Water Masking

Because the wet component obtained by tasseled cap transformation is mainly associated with the humidity of vegetation and soil [54] and because RSEI is more suitable for land surfaces than for large water areas, water bodies should be masked out from the images of the study area. Considering that official water boundaries are not always available for historical water bodies and mostly do not contain small water bodies but large ones such as rivers and lakes, it was decided to apply the modified normalized difference water index (MNDWI) [14] to mask out water bodies in the study area.

$$\text{MNDWI} = \frac{\rho_{\text{green}} - \rho_{\text{SWIR1}}}{\rho_{\text{green}} + \rho_{\text{SWIR1}}} \quad (10)$$

where ρ_{green} and ρ_{SWIR1} are the reflectance in the green and SWIR1 bands of Landsat image respectively.

3.3.3. Integration of the Measures

Regarding how the RSEI model was constructed, Xu et al. [14] excluded traditional weight-based methods such as the analytic hierarchy process (AHP) because bias based on the researcher's own knowledge background might be introduced and proposed the use of principal component analysis (PCA). Through PCA, most of the normalized measures are explained by the first principal component (PC1). For this reason, PC1 can be used to represent the RSEI. The importance of each normalized measure is weighted by their respective loadings to PC1:

$$\text{RSEI} = \text{PC1} = a \times \text{nNDVI} + b \times \text{nWetness} + c \times \text{nNDBSI} + d \times \text{nLSI} \quad (11)$$

where a , b , c , and d , are the loadings of the normalized measures to PC1 obtained by decomposing the covariance matrix, which could be used as their corresponding weights for calculating RSEI. PC1 is the largest contributing eigenvector obtained by integrating multidimensional measures through principal component analysis, and its contribution can often reach over 80% [14]. However, it is noted that the above weights vary with imagery, which does not allow a direct comparison of multitemporal RSEI [22]. To address this concern, we utilized a simple method to determine the weights for seasonal RSEI [22]. For example, the weights for spring are given by:

$$a_{\text{spring}} = \frac{a_{1992 \text{ spring}} + a_{2005 \text{ spring}} + a_{2018 \text{ spring}}}{3} \quad (12)$$

a_{spring} is the average of the spring nNDVI weights over the 3 years. The weights for summer, autumn, and winter can be obtained similarly.

The resultant RSEI was also normalized to the 0–1 range. As such, a higher RSEI value indicates better eco-environment quality and vice versa. After the generation of seasonal RSEI maps, annual RSEI maps were produced by averaging four respective seasonal RSEI maps. For a comparative analysis, RSEI was classified into five levels, namely 0.0–0.2 (Poor), 0.2–0.4 (Fair), 0.4–0.6 (Moderate), 0.6–0.8 (Good) and 0.8–1.0 (Excellent) using the equal interval classification method like [14,27,55]. This method allows data produced in different years to be directly compared for a multitemporal analysis [14,27].

4. Results and Discussion

Before analyzing the results, it is still important to emphasize that the data used in this study are not perfect and not very representative, but it is the best solution given various constraints.

4.1. RSEI Indicators

With the methods described in Section 3.2, RSEI indicators were derived and their mean values of the entire study area in each season of each year are shown in Figure 3. The seasonal variability of these measures is clear from Figure 3. While NDVI, wetness, and LST initially increased and then decreased over the season, NDBSI showed an opposite trend. Autumn saw the highest NDVI and wetness but the lowest NDBSI. Not surprisingly, the highest LST occurred in summer. Annually, these measures did not show a simple increasing or decreasing trend but, obviously, the measures in 2018 were mostly higher than in earlier years.

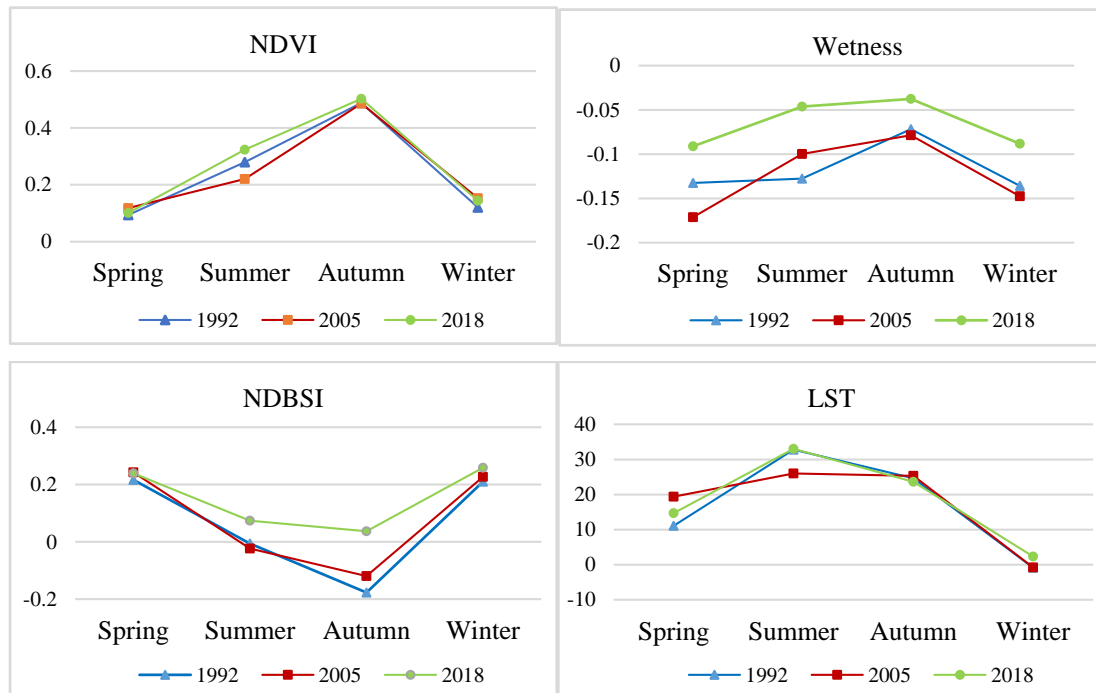


Figure 3. Average normalized difference vegetation index (NDVI), Wetness, normalized difference building-soil index (NDBSI), and land surface temperature (LST) of the study area in each season of each year.

The results of the correlation analysis are shown in Table 3. Correlation between NDVI and other measures differed between the four seasons. NDVI was positively correlated with wetness in warm seasons (summer and autumn) but negatively in cool seasons (spring and winter). However, NDVI was negatively correlated with NDBSI and LST in warm seasons but positively in cool seasons. Obviously, the distribution of positive and negative values in spring and winter is different from that in summer and autumn. This suggests that the contributions of wetness, dryness, and heat to urban eco-environment quality vary with the season. This finding is different from previous studies [14,17,55] that assumed a fixed contribution.

Figure 4 illustrates the different distributions of the four normalized measures in spring and winter compared with summer and autumn in Tianjin. As the normalization method for the measures depends on the correlations shown in Table 3, to avoid repeating such observations, autumn and winter 2005 were selected separately from the seasons in which the same normalization method was applied for presentation.

Table 3. Correlations between NDVI and other measures.

Year	Measure	Spring	Summer	Autumn	Winter
1992	Wetness	−0.297	0.391	0.231	−0.405
	NDBSI	0.161	−0.660	−0.742	0.264
	LST	0.062	−0.439	−0.624	0.251
2005	Wetness	−0.276	0.503	0.327	−0.221
	NDBSI	0.302	−0.826	−0.701	0.082
	LST	0.140	−0.497	−0.357	0.177
2018	Wetness	−0.339	0.617	0.322	−0.101
	NDBSI	0.377	−0.808	−0.457	0.018
	LST	0.024	−0.432	−0.518	0.221

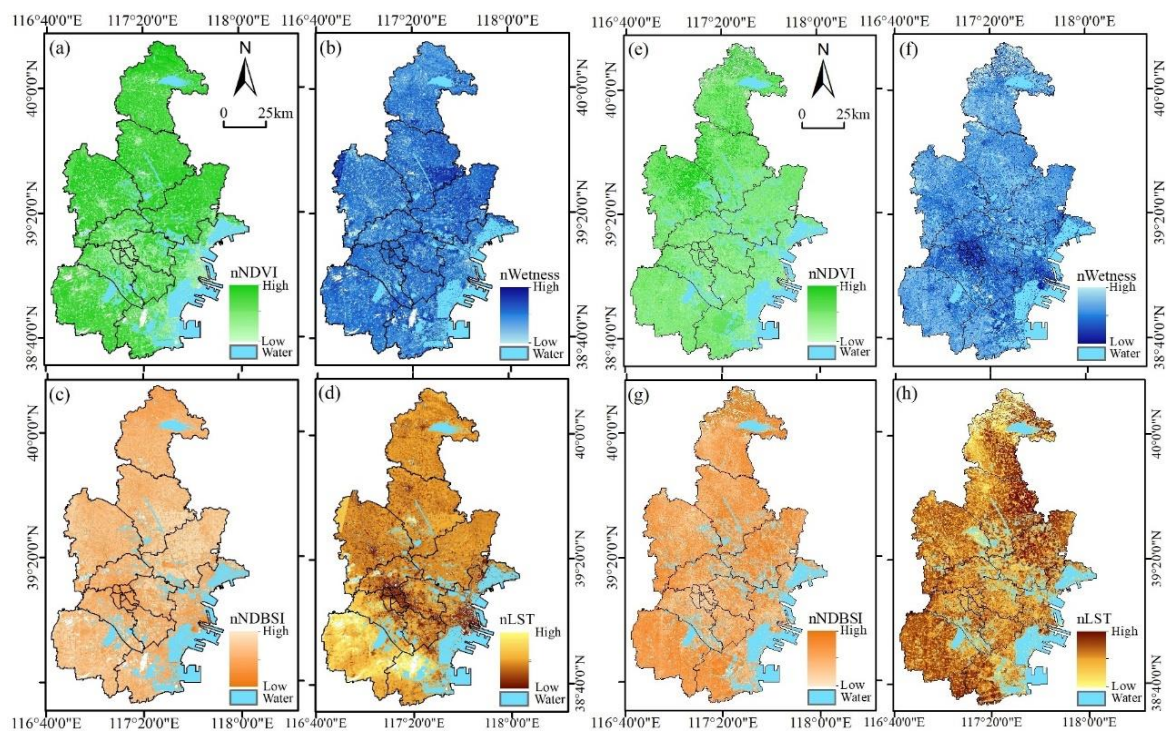


Figure 4. Normalized NDVI for the greenness, normalized wetness for the moisture, normalized NDBSI for the dryness, and normalized LST for the heat of the study area. (a–d) for autumn 2005 and (e–h) for winter 2005. Note that as a result of the application of different normalization processes the color representing the minimal or maximal values varies with the season for nWetness, nNDBSI, and nLST.

On the normalized NDVI maps (Figure 4a,c), nNDVI values were relatively low in the Central Urban Area regardless of period, which could be attributed to less vegetation in that area. The entire study area was greener in September than in December. This is consistent with seasonal climatic variability in Tianjin: the September climate is more suitable for vegetation growth while a dry and cold December is usually detrimental to plants and, therefore, causes a remarkable reduction in vegetation. Interestingly, the lower nWetness values in the Central Urban Area show that it was moister than most of the other areas in December (Figure 4f). As for dryness (Figure 4c) and heat (Figure 4d), they were higher in the Central Urban Area than in other areas in September, which agrees with previous studies [16,55]. However, that is not the case for December when the other areas were drier and warmer than the Central Urban Area. We believe that this might be related to the dry farmland in the suburban areas of the city in spring and winter. Although there was wheat coverage in the two seasons, they did not help to cool and moisturize. In the

heat image of September 2005 (Figure 4d), there was a lower temperature zone in southern Tianjin because of a thin layer of clouds.

4.2. RSEI Distribution

By using the method described in Section 3.3.3 for integrating the measures, we calculated the annual RSEI values of the study area. The RSEI level maps were generated (Figure 5) and statistical analysis was also performed (Table 4). Overall, most of Tianjin were at the moderate (0.4–0.6) and good (0.6–0.8) RSEI levels with only small portions (all <1%) at the poor (0.0–0.2) and excellent (0.8–1.0) levels. It is interesting to notice that the Central Urban Area remained at the moderate level (0.4–0.6) throughout the 26 years. These results are similar to an assessment of ecological security in the Beijing–Tianjin–Hebei region for the period 2000–2015 using the ecological security index, which concluded that Tianjin’s security coefficient was above 0.8 per year, the highest level in the region, and that Tianjin has maintained a high level of ecological quality [14].

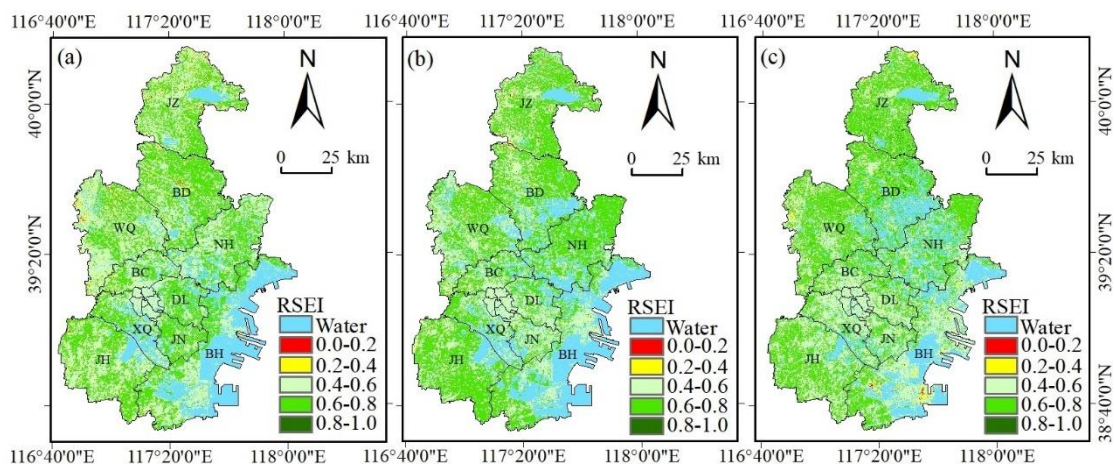


Figure 5. The RSEI level maps of 1992 (a), 2005 (b), and 2018 (c). The Binhai New Area in the 2018 image has a large amount of area that is not covered by water compared to the other two images, which is due to the reclamation of the sea in recent years to. Land areas close the sea particularly in the Binhai New Area were covered by water in 1992 and 2005 but appeared in 2018 because of dock construction completed in recent years.

Table 4. The area of each RSEI grade. Note that the total area varied with years because water areas changed over time and were removed by water masking (Section 3.3.2).

RSEI Grade	1992		2005		2018	
	Area/km ²	%	Area/km ²	%	Area/km ²	%
Poor (0–0.2)	36.5	0.380	24.6	0.271	30.9	0.328
Fair (0.2–0.4)	256.9	2.670	205.9	2.264	189.1	2.007
Moderate (0.4–0.6)	5124.7	53.271	4057.5	44.613	4501.9	47.773
Good (0.6–0.8)	4199.9	43.658	4806.6	52.850	4671.4	49.571
Excellent (0.8–1)	2.0	0.022	0.2	0.002	30.3	0.321
Total	9620.03	100	9094.79	100	9423.66	100

In 1992, the moderate RSEI level areas (53.271%) were mostly concentrated in Baodi and Wuqing, 9.613% more than the good level areas. The red area means the worst eco-environmental quality area, which is evident in the center of the Baodi district, and we believe this is related to the mining activity in the district during this period, which is shown on the original image as an area covered in bare soil. The poor-level area was also found in Baodi, which we believe might be associated with the then mining activity in that district. In 2005, the entire study area was dominated by the good level (52.850%), 8.237% higher than the moderate level, which was largely found in the Around-Center Area. This

suggests that the urban expansion in this area began in the 2000s. In addition, the red areas of the period are not obvious and are mostly scattered and difficult to analyze. In 2018, the percentage difference between the moderate- and the good-level areas declined to only 1.798%. Meanwhile, in the southern part of the Binhai New Area there is a distinctly clustered red area, which, as seen through the original image, originates from a bare patch of land that had just been created by the completion of reclamation. Despite the continued urban expansion and sea reclamation the local government's relentless efforts to protect the environment in the meanwhile helped moderate the difference.

4.3. RSEI Change

4.3.1. Seasonal and Annual RSEI Change

Seasonal and annual RSEI values were calculated for temporal analysis (Figure 6). Within each year, RSEI changed over season, initially declining sharply and then rising gradually with the lowest values in summer and highest in winter. Seasonal RSEI did not change much during the 26 years except for the summer RSEI—which increased gradually from 0.456 in 1992 to 0.545 in 2018. Overall, the annual RSEI increased slightly from 0.518 in 1992 to 0.597 in 2018, which indicates a steady improvement in the eco-environmental conditions in Tianjin. This is consistent with the results reported by Yue et al. [37] who assessed Tianjin's ecosystem using a different index. This may be related to Tianjin's recent implementation of the two-city green space ecological barrier project and the Sino-Singapore Tianjin Eco-city project. In addition to greening efforts in the city, these projects also contributed to wetland restoration and improved water systems and settlement environment. Although water bodies were masked out in the RSEI assessment, the expansion of urban water bodies has been reported to effectively lower surrounding temperatures [56], thereby improving the urban eco-environment.

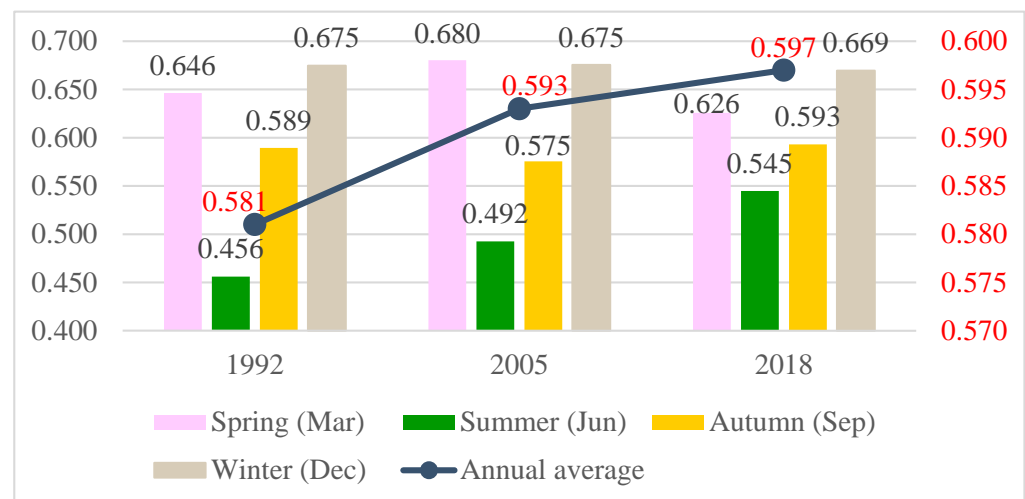


Figure 6. Changes in average seasonal and annual RSEI of the study area.

The interesting changes in the average seasonal and annual RSEI illustrated in Figure 6 highlight the importance of using more remote sensing images rather than less in RSEI-based assessment. If only spring images were used, it would be concluded that the urban eco-environment quality first improved and then deteriorated; if only summer images were used, we might find a gradual improvement in the urban eco-environment quality; if only autumn images were used, it would be easy to claim that the urban eco-environment quality first declined and then improved; if only winter images were used, we might believe that there was almost no change. However, when we examine the annual RSEI change, the finding is similar to that in the case of summer images only. This implies that the selection of remote-sensing images for representing the entire years' eco-environmental conditions could produce various results, thus confusing decision-makers. Performing

a multitemporal analysis using satellite image data often requires us to consider how frequently remotely sensed variables change over time [57]. For example, land-use/-cover changes every 1–10 years and there is limited monthly or seasonal change except for the phenological cycles of vegetation) so it is acceptable to examine land-use/-cover change with several (mosaicked) images acquired in the same or near dates but in different years [58–60]. However, the remotely sensed variables (NDVI, Wetness, NDBSI, and LST) for deriving RSEI can change seasonally, monthly, and even daily and a single day's eco-environmental condition is insufficient for representing an entire year's. For this reason, it is advisable to avoid such a practice, which is often found in many studies [14,17,55,61], and to use as many remote-sensing images as possible to characterize a year's eco-environmental condition, which helps produce a more reliable assessment result.

4.3.2. Spatial Distribution of RSEI Change

The spatial distribution of RSEI change from 1992–2005, 2005–2018, and 1992–2018 is shown in Figure 7 and statistical analysis was also performed (Table 5). In the three maps of Figure 7, the Central Urban Area that remained mostly white and other districts such as Jizhou, and Baodi, and Wuqing that had large white areas accounted for the majority of the no-change area in Table 5.

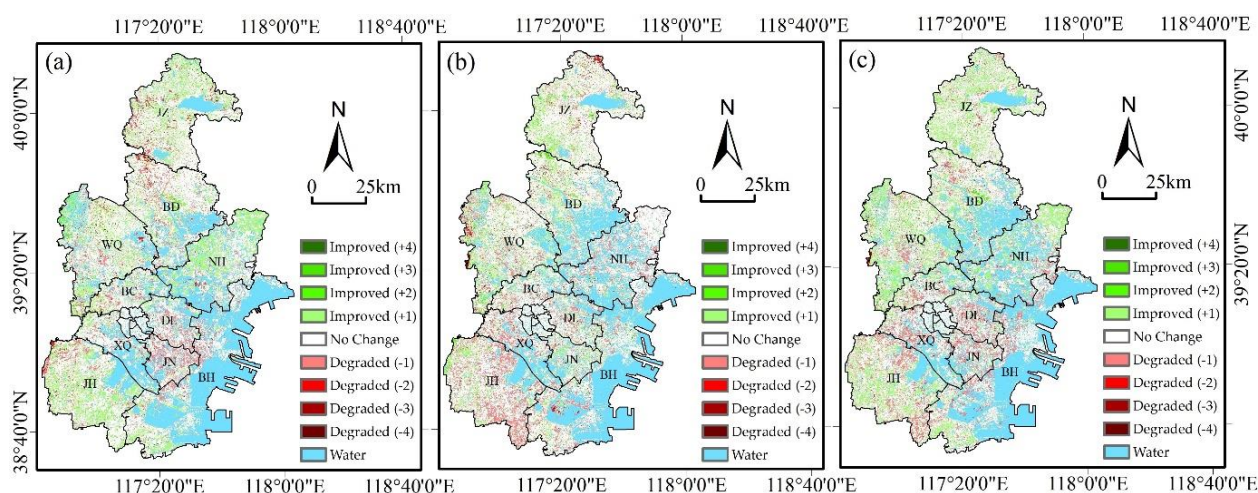


Figure 7. RSEI level change maps from 1992–2005 (a), 2005–2018 (b), and 1992–2018 (c). The legend means a change in the RSEI level over a period. For example, Change (+2) means that the RSEI level of a given area represented by a pixel increased by two levels, e.g., from Poor to Moderate.

Table 5. The total area of each change in Tianjin.

Class	Change	1992–2005		2005–2018		1992–2018	
		Class Area/km ²	Change Area/km ²	Class Area/km ²	Change Area/km ²	Class Area/km ²	Change Area/km ²
Degraded	−4		1.23		6.15		1.10
	−3	1082.63	19.22	1404.46	31.64	1347.42	15.88
	−2	(12.61%)	144.85	(17.00%)	117.98	(16.02%)	98.46
	−1		917.32		1248.70		2108.88
No change	0	5521.98	5521.98	5410.78	5410.78	4838.96	4838.96
		(64.31%)		(65.50%)		(57.53%)	
Improved	1		1764.56		1246.93		1274.81
	2	1981.43	189.78	1445.25	175.03	2224.32	45.35
	3	(23.08%)	26.67	(17.50%)	22.65	(26.45%)	20.62
	4		0.42		0.63		6.64

From 1992 to 2015 (Figure 7a), the improved areas (23.08%) were 10.47% more than the degraded areas (12.61%) (Table 5). It is noted that most of Jinan and Dongli, which connect the Central Urban Area and the Binhai New Area, saw an obvious eco-environmental degradation, which resulted from urbanization in these areas during the period [62]. This situation, however, seemed to have changed from 2015 to 2018 (Figure 7b). In particular, most of Jinnan showed an eco-environmental improvement as a result of the construction of Tianjin's two-city green space ecological barrier project [63]. As available land resources in the area between the Central Urban Area and the Binhai New Area became decreasingly available, the demand for land then moved to southwestern Tianjin rose. Although eco-environmental protection measures were in place in these areas, apparently they were not as effective as a major project like the two-city green space ecological barrier project [62]. This explains why eco-environmental degradation was considerable in both Xiqing and Jinghai. As a result, the recent 13 years saw a smaller difference between the improved area (17.50%) and the degraded area (17.00%) (Table 5). The overall 26-year change (Figure 7c) shows that the overall eco-environment quality of the Remote Suburbs Area was improving, while most of the Around-Center Area was at the degradation level (−1), which indicates that the occupation of the built-up urban areas in this area still caused a slight ecological degradation in general, but without environmental protection measures, it is believed that the eco-environmental quality of these areas would be even worse. This is evident in a study examining urban sprawl in Beijing, Tianjin, and Shijiazhuang, which calculates a normalized annual urban growth rate of 5.2 for Tianjin from 1990 to 2010, much greater than Beijing's 3.6 and Shijiazhuang's 4.0 [62].

To unravel the characteristics of RSEI change on a district scale, we plotted the RSEI values of the 16 districts grouped in four categories (Figure 8). The RSEI value of the Central Urban Area was always lower than the other three areas during the 26 years. This is not surprising, considering the high-density impervious surfaces in this populated part of the city. Despite the fluctuation, the RSEI of this area increased in recent years compared with 1992. Among the districts in the Around-Center Area, RSEI changes were considerable and generally positive except for Beichen. The districts in the Remote Suburb Area also had overall increasing RSEI values from 1992–2018 but with some decreases in the recent 13 years. The change for the Binhai New Area was constantly negative through the 26 years. We assume that urban expansion in the area and bare land created from sea reclamation programs during the period were responsible for such eco-environmental degradation.

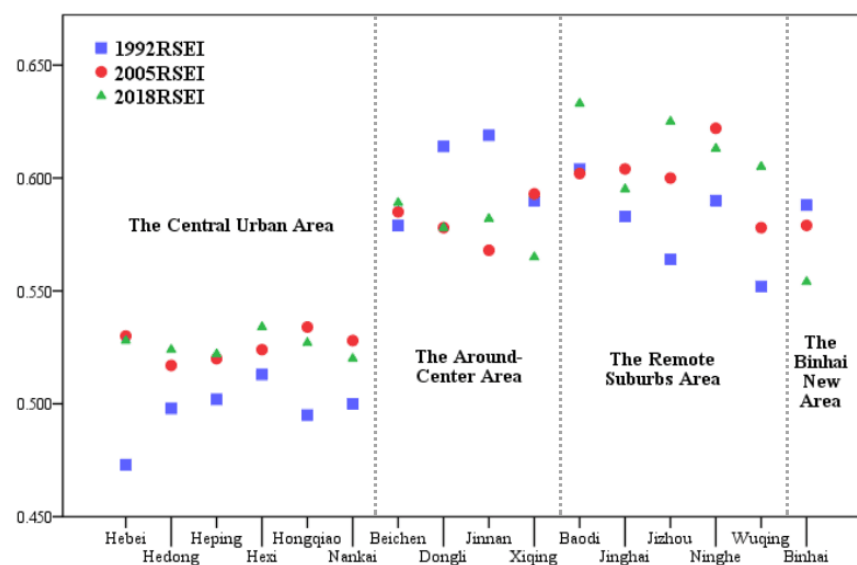


Figure 8. RSEI change in each district from 1992–2018.

4.4. Innovations and Limitations

The highlight of this study is improving the reliability of urban eco-environment quality assessment by considering seasonal variability in both the contributions of RSEI indicators to eco-environment quality and RSEI values. Although it is claimed that greenness and wetness positively and heat and dryness negatively impact eco-environmental conditions [22], this study reveals that their impacts vary with the season. As such, this helps determine how RSEI indicator measures should be normalized accordingly. Also, previous RSEI studies [14,17,55] used the remote-sensing images acquired mostly between April to October and assumed that RSEI from such a biased selection of images could be sufficient for characterizing annual urban eco-environmental conditions. However, our finding shows that this is not the case—RSEI varies from month to month and season to season. More remote-sensing images are therefore needed for representing seasonal and annual RSEI.

However, we also would like to note the limitations of the study. As mentioned in Section 3.1, the selection of remote-sensing images in this study was not ideal. We believe that the urban eco-environmental quality assessment would be improved if better (in terms of timing) and more images (e.g., one image for every month) had been used. In addition, like other RSEI studies [14,17,55], water bodies are masked out, limiting the assessment to land surfaces. An avenue for future work might be including them to complete the area examined in the assessment.

5. Conclusions

This study proposes a new RSEI-based urban eco-environment quality assessment method by considering seasonal variability and tests it in Tianjin with remote-sensing images acquired in four seasons of 1992, 2005, and 2018. The key findings and main conclusions are summarized as follows:

- Both the contributions of RSEI indicators to eco-environment quality and RSEI values vary with the season. Such seasonal variability should be considered normalizing indicator measures differently and using more remote-sensing images respectively to improve the assessment.
- Though with rapid urban expansion, Tianjin maintained a gradual urban eco-environment quality improvement over the 26 years from 1992 to 2018. This could be explained by the implementation of projects that increased urban green space.
- The most recent 13 years saw improved eco-environmental conditions in the joint area between the Central Urban Area and the Binhai New Area from eco-environmental restoration but these also gradually deteriorated in the Binhai New Area due to urban expansion and sea reclamation.

The method proposed in this study proves to be a viable tool for environmental researchers and managers that produces more reliable assessment, thus gaining a more accurate understanding of the evolution of the urban eco-environment quality over time. For a multi-temporal analysis, we encourage use of as many remote-sensing images as possible that represent monthly or seasonal eco-environmental conditions. In the meantime, we suggest that the decision makers in Tianjin pay attention to the ecological protection of Xiqing District and Binhai New Area and that ecological planning should be incorporated in land reclamation projects.

Author Contributions: Conceptualization, Ruiqing Yang, Ting Zhang and Long Li; methodology, Ruiqing Yang, Ting Zhang, Yibo Yang and Long Li; software, Ruiqing Yang, Ting Zhang and Yibo Yang; validation, Ruiqing Yang and Ting Zhang; formal analysis, Ruiqing Yang and Ting Zhang; investigation, Ruiqing Yang, Ting Zhang and Yibo Yang; resources, Long Li and Longqian Chen; data curation, Ruiqing Yang, Ting Zhang and Yibo Yang; writing—original draft preparation, Ruiqing Yang, Ting Zhang and Yibo Yang; writing—review and editing, Long Li and Longqian Chen; visualization, Ruiqing Yang and Ting Zhang; supervision, Long Li and Longqian Chen; project administration,

Long Li and Longqian Chen; funding acquisition, Ting Zhang, Long Li and Longqian Chen. All authors have read and agreed to the published version of the manuscript.

Funding: This research was supported by “the Fundamental Research Funds for the Central Universities” (Grant No.: 2018QNB06).

Institutional Review Board Statement: Not applicable.

Informed Consent Statement: Not applicable.

Data Availability Statement: Data are available from the corresponding author upon reasonable request.

Acknowledgments: The authors would like to thank the United States Geological Survey (USGS) and the China Meteorological Administration for freely providing Landsat data and weather data, respectively. The authors would also like to thank Junyu Zhao with the China University of Mining and Technology for his assistance in the early stage of the work and four anonymous reviewers for their constructive comments that helped to improve the article.

Conflicts of Interest: The authors declare no conflict of interest.

References

- Schneider, A. Monitoring land cover change in urban and peri-urban areas using dense time stacks of Landsat satellite data and a data mining approach. *Remote Sens. Environ.* **2012**, *124*, 689–704. [\[CrossRef\]](#)
- Wolch, J.R.; Byrne, J.; Newell, J.P. Urban green space, public health, and environmental justice: The challenge of making cities “just green enough.”. *Landsc. Urban Plan.* **2014**, *125*, 234–244. [\[CrossRef\]](#)
- Firozjaei, M.K.; Fathololomi, S.; Kiavarz, M.; Arsanjani, J.J.; Homae, M.; Alavipanah, S.K. Modeling the impact of the COVID-19 lockdowns on urban surface ecological status: A case study of Milan and Wuhan cities. *J. Environ. Manag.* **2021**, *286*, 112236. [\[CrossRef\]](#)
- Li, Y.; Jia, L.; Wu, W.; Yan, J.; Liu, Y. Urbanization for rural sustainability—Rethinking China’s urbanization strategy. *J. Clean. Prod.* **2018**, *178*, 580–586. [\[CrossRef\]](#)
- Psomiadis, E.; Papazachariou, A.; Soulis, K.X.; Alexiou, D.S.; Charalampopoulos, I. Landslide mapping and susceptibility assessment using geospatial analysis and earth observation data. *Land* **2020**, *9*, 133. [\[CrossRef\]](#)
- Kouli, M.; Loupasakis, C.; Soupios, P.; Vallianatos, F. Landslide hazard zonation in high risk areas of Rethymno Prefecture, Crete Island, Greece. *Nat. Hazards* **2010**, *52*, 599–621. [\[CrossRef\]](#)
- Kumar, P.; Thakur, P.K.; Bansod, B.K.; Debnath, S.K. Multi-criteria evaluation of hydro-geological and anthropogenic parameters for the groundwater vulnerability assessment. *Environ. Monit. Assess.* **2017**, *189*, 564. [\[CrossRef\]](#)
- Willis, K.S. Remote sensing change detection for ecological monitoring in United States protected areas. *Biol. Conserv.* **2015**, *182*, 233–242. [\[CrossRef\]](#)
- He, F.; Gu, L.; Wang, T.; Zhang, Z. The synthetic geo-ecological environmental evaluation of a coastal coal-mining city using spatiotemporal big data: A case study in Longkou, China. *J. Clean. Prod.* **2017**, *142*, 854–866. [\[CrossRef\]](#)
- Li, S.; Bing, Z.; Jin, G. Spatially explicit mapping of soil conservation service in monetary units due to land use/cover change for the three gorges reservoir area, China. *Remote Sens.* **2019**, *11*, 468. [\[CrossRef\]](#)
- Zhang, L.; Liu, L.; Xia, Z.; Li, W.; Fan, Q. Sparse trajectory prediction based on multiple entropy measures. *Entropy* **2016**, *18*, 327. [\[CrossRef\]](#)
- Li, J.; Song, C.; Cao, L.; Zhu, F.; Meng, X.; Wu, J. Impacts of landscape structure on surface urban heat islands: A case study of Shanghai, China. *Remote Sens. Environ.* **2011**, *115*, 3249–3263. [\[CrossRef\]](#)
- Buyantuyev, A.; Wu, J. Urban heat islands and landscape heterogeneity: Linking spatiotemporal variations in surface temperatures to land-cover and socioeconomic patterns. *Landsc. Ecol.* **2010**, *25*, 17–33. [\[CrossRef\]](#)
- Xu, H.; Wang, M.; Shi, T.; Guan, H.; Fang, C.; Lin, Z. Prediction of ecological effects of potential population and impervious surface increases using a remote sensing based ecological index (RSEI). *Ecol. Indic.* **2018**, *93*, 730–740. [\[CrossRef\]](#)
- Xu, H.; Wang, Y.; Guan, H.; Shi, T.; Hu, X. Detecting ecological changes with a remote sensing based ecological index (RSEI) produced time series and change vector analysis. *Remote Sens.* **2019**, *11*, 2345. [\[CrossRef\]](#)
- Hu, X.; Xu, H. A new remote sensing index based on the pressure-state-response framework to assess regional ecological change. *Environ. Sci. Pollut. Res.* **2019**, *26*, 5381–5393. [\[CrossRef\]](#)
- Hu, X.; Xu, H. A new remote sensing index for assessing the spatial heterogeneity in urban ecological quality: A case from Fuzhou City, China. *Ecol. Indic.* **2018**, *89*, 11–21. [\[CrossRef\]](#)
- Shan, W.; Jin, X.; Ren, J.; Wang, Y.; Xu, Z.; Fan, Y.; Gu, Z.; Hong, C.; Lin, J.; Zhou, Y. Ecological environment quality assessment based on remote sensing data for land consolidation. *J. Clean. Prod.* **2019**, *239*, 118126. [\[CrossRef\]](#)
- Wen, X.; Ming, Y.; Gao, Y.; Hu, X. Dynamic monitoring and analysis of ecological quality of pingtan comprehensive experimental zone, a new type of sea island city, based on RSEI. *Sustainability* **2020**, *12*, 21. [\[CrossRef\]](#)
- Ji, J.; Wang, S.; Zhou, Y.; Liu, W.; Wang, L. Studying the Eco-Environmental Quality Variations of Jing-Jin-Ji Urban Agglomeration and Its Driving Factors in Different Ecosystem Service Regions from 2001 to 2015. *IEEE Access* **2020**, *8*, 154940–154952. [\[CrossRef\]](#)

21. Zhou, Z.; Du, J.; Liu, Y. Evolution, development and evaluation of eco-transportation in Guangdong-Hong Kong-Macao Greater Bay Area. *Syst. Sci. Control. Eng.* **2020**, *8*, 97–107. [CrossRef]
22. Wang, B.; Chen, L.; Li, L.; Xie, H.; Zhang, Y. Ecological response to land use change: A case study from the Chaohu lake basin, China. *Bulg. Chem. Commun.* **2017**, *49*, 200–206.
23. Guo, B.; Fang, Y.; Jin, X.; Zhou, Y. Monitoring the effects of land consolidation on the ecological environmental quality based on remote sensing: A case study of Chaohu Lake Basin, China. *Land Use Policy* **2020**, *95*, 104569. [CrossRef]
24. Li, Y.; Wu, L.; Han, Q.; Wang, X.; Zou, T.; Fan, C. Estimation of remote sensing based ecological index along the Grand Canal based on PCA-AHP-TOPSIS methodology. *Ecol. Indic.* **2021**, *122*, 107214. [CrossRef]
25. Liao, W.; Jiang, W. Evaluation of the spatiotemporal variations in the eco-environmental quality in China based on the remote sensing ecological index. *Remote Sens.* **2020**, *12*, 2462. [CrossRef]
26. Qureshi, S.; Alavipanah, S.K.; Konyushkova, M.; Mijani, N.; Fathololomi, S.; Firozjaei, M.K.; Homae, M.; Hamzeh, S.; Kakroodi, A.A. A remotely sensed assessment of surface ecological change over the Gomishan Wetland, Iran. *Remote Sens.* **2020**, *12*, 2989. [CrossRef]
27. Boori, M.S.; Choudhary, K.; Paringer, R.; Kupriyanov, A. Spatiotemporal ecological vulnerability analysis with statistical correlation based on satellite remote sensing in Samara, Russia. *J. Environ. Manag.* **2021**, *285*, 112138. [CrossRef]
28. Firozjaei, M.K.; Kiavarz, M.; Homae, M.; Arsanjani, J.J.; Alavipanah, S.K. A novel method to quantify urban surface ecological poorness zone: A case study of several European cities. *Sci. Total Environ.* **2021**, *757*, 143755. [CrossRef]
29. Karimi Firozjaei, M.; Fathololoumi, S.; Kiavarz, M.; Biswas, A.; Homae, M.; Alavipanah, S.K. Land Surface Ecological Status Composition Index (LSESCI): A novel remote sensing-based technique for modeling land surface ecological status. *Ecol. Indic.* **2021**, *123*, 107375. [CrossRef]
30. Yue, H.; Liu, Y.; Li, Y.; Lu, Y. Eco-environmental quality assessment in china's 35 major cities based on remote sensing ecological index. *IEEE Access* **2019**, *7*, 51295–51311. [CrossRef]
31. Seddon, A.W.R.; Macias-Fauria, M.; Long, P.R.; Benz, D.; Willis, K.J. Sensitivity of global terrestrial ecosystems to climate variability. *Nature* **2016**, *531*, 229–232. [CrossRef]
32. Tianjin Weather. Available online: <https://weather.cma.cn/web/weather/54517> (accessed on 11 May 2021).
33. Yi, P.; Li, W.; Zhang, D. Sustainability assessment and key factors identification of first-tier cities in China. *J. Clean. Prod.* **2021**, *281*, 125369. [CrossRef]
34. 2019 Official List of New First-Tier Cities: Where Does Your City Rank? Available online: <https://www.yicai.com/news/100200192.html> (accessed on 11 May 2021).
35. Tianjin Municipal People's Government. *Tianjin Economic Yearbook 1992*, 1st ed.; Tianjin Statistical Yearbooks Press: Tianjin, China, 1992; p. 700.
36. Tianjin Municipal People's Government. *Yearbook of Tianjin 2019*, 1st ed.; Tianjin Statistical Yearbooks Press: Tianjin, China, 2019; p. 50.
37. Yue, S.; Yang, Y.; Pu, Z. Total-factor ecology efficiency of regions in China. *Ecol. Indic.* **2017**, *73*, 284–292. [CrossRef]
38. Mishra, N.; Haque, M.O.; Leigh, L.; Aaron, D.; Helder, D.; Markham, B. Radiometric cross calibration of landsat 8 Operational Land Imager (OLI) and landsat 7 enhanced thematic mapper plus (ETM+). *Remote Sens.* **2014**, *6*, 12619–12638. [CrossRef]
39. Koutsias, N.; Pleniou, M. Comparing the spectral signal of burned surfaces between Landsat 7 ETM+ and Landsat 8 OLI sensors. *Int. J. Remote Sens.* **2015**, *36*, 3714–3732. [CrossRef]
40. Rouse, J.W.; Haas, R.H.; Scheel, J.A.; Deering, D.W. Monitoring Vegetation Systems in the Great Plains with ERTS. *Proc. Third ERTS Symp.* **1973**, *1*, 48–62.
41. Li, L.; Bakelants, L.; Solana, C.; Canters, F.; Kervyn, M. Dating lava flows of tropical volcanoes by means of spatial modeling of vegetation recovery. *Earth Surf. Process. Landf.* **2018**, *43*, 840–856. [CrossRef]
42. Zhou, X.; Li, L.; Chen, L.; Liu, Y.; Cui, Y.; Zhang, Y.; Zhang, T. Discriminating urban forest types from Sentinel-2A image data through linear spectral mixture analysis: A case study of Xuzhou, East China. *Forests* **2019**, *10*, 478. [CrossRef]
43. Li, L.; Zhou, X.; Chen, L.; Chen, L.; Zhang, Y.; Liu, Y. Estimating urban vegetation biomass from sentinel-2A image data. *Forests* **2020**, *11*, 125. [CrossRef]
44. Crist, E.P. A TM Tasseled Cap equivalent transformation for reflectance factor data. *Remote Sens. Environ.* **1985**, *17*, 301–306. [CrossRef]
45. Baig, M.H.A.; Zhang, L.; Shuai, T.; Tong, Q. Derivation of a tasseled cap transformation based on Landsat 8 at-satellite reflectance. *Remote Sens. Lett.* **2014**, *5*, 423–431. [CrossRef]
46. Xu, H. A new index for delineating built-up land features in satellite imagery. *Int. J. Remote Sens.* **2008**, *29*, 4269–4276. [CrossRef]
47. Essa, W.; Verbeiren, B.; van der Kwast, J.; Van de Voorde, T.; Batelaan, O. Evaluation of the DisTrad thermal sharpening methodology for urban areas. *Int. J. Appl. Earth Obs. Geoinf.* **2012**, *19*, 163–172. [CrossRef]
48. Jimenez-Munoz, J.C.; Cristobal, J.; Sobrino, J.A.; Soria, G.; Ninyerola, M.; Pons, X. Revision of the single-channel algorithm for land surface temperature retrieval from landsat thermal-infrared data. *IEEE Trans. Geosci. Remote Sens.* **2009**, *47*, 339–349. [CrossRef]
49. Sobrino, J.A.; Jiménez-Muñoz, J.C.; Paolini, L. Land surface temperature retrieval from LANDSAT TM 5. *Remote Sens. Environ.* **2004**, *90*, 434–440. [CrossRef]

50. Weng, Q. Thermal infrared remote sensing for urban climate and environmental studies: Methods, applications, and trends. *ISPRS J. Photogramm. Remote Sens.* **2009**, *64*, 335–344. [[CrossRef](#)]
51. Nichol, J. Remote sensing of urban heat islands by day and night. *Photogramm. Eng. Remote Sens.* **2005**, *71*, 613–621. [[CrossRef](#)]
52. Liu, W.; Li, L.; Chen, L.; Wen, M.; Wang, J.; Yuan, L.; Liu, Y.; Li, H. Testing a comprehensive volcanic risk assessment of tenerife by volcanic hazard simulations and social vulnerability analysis. *ISPRS Int. J. Geo-Inf.* **2020**, *9*, 273. [[CrossRef](#)]
53. Yang, C.; Zeng, W.; Yang, X. Coupling coordination evaluation and sustainable development pattern of geo-ecological environment and urbanization in Chongqing municipality, China. *Sustain. Cities Soc.* **2020**, *61*, 102271. [[CrossRef](#)]
54. Mostafiz, C.; Chang, N.-B. Tasseled cap transformation for assessing hurricane landfall impact on a coastal watershed. *Int. J. Appl. Earth Obs. Geoinf.* **2018**, *73*, 736–745. [[CrossRef](#)]
55. Yuan, B.; Fu, L.; Zou, Y.; Zhang, S.; Chen, X.; Li, F.; Deng, Z.; Xie, Y. Spatiotemporal change detection of ecological quality and the associated affecting factors in Dongting Lake Basin, based on RSEI. *J. Clean. Prod.* **2021**, *302*, 126995. [[CrossRef](#)]
56. Sun, X.; Tan, X.; Chen, K.; Song, S.; Zhu, X.; Hou, D. Quantifying landscape-metrics impacts on urban green-spaces and water-bodies cooling effect: The study of Nanjing, China. *Urban For. Urban Green.* **2020**, *55*, 126838. [[CrossRef](#)]
57. Jensen, J.R. Remote Sensing of the Environment. In *Remote Sensing of the Environment: Pearson New International Edition: An Earth Resource Perspective*, 2nd ed.; Pearson Education Limited: Essex, UK, 2013; pp. 17–19.
58. Cui, Y.; Li, L.; Chen, L.; Zhang, Y.; Cheng, L.; Zhou, X.; Yang, X. Land-use carbon emissions estimation for the Yangtze River Delta Urban Agglomeration using 1994–2016 Landsat image data. *Remote Sens.* **2018**, *10*, 1334. [[CrossRef](#)]
59. Li, H.; Li, L.; Chen, L.; Zhou, X.; Cui, Y.; Liu, Y.; Liu, W. Mapping and characterizing spatiotemporal dynamics of impervious surfaces using landsat images: A case study of Xuzhou, East China from 1995 to 2018. *Sustainability* **2019**, *11*, 1224. [[CrossRef](#)]
60. Hu, S.; Chen, L.; Li, L.; Zhang, T.; Yuan, L.; Cheng, L.; Wang, J.; Wen, M. Simulation of land use change and ecosystem service value dynamics under ecological constraints in Anhui province, China. *Int. J. Environ. Res. Public Health* **2020**, *17*, 4228. [[CrossRef](#)] [[PubMed](#)]
61. Yunus, A.P.; Fan, X.; Tang, X.; Jie, D.; Xu, Q.; Huang, R. Decadal vegetation succession from MODIS reveals the spatio-temporal evolution of post-seismic landsliding after the 2008 Wenchuan earthquake. *Remote Sens. Environ.* **2020**, *236*, 111476. [[CrossRef](#)]
62. Wu, W.; Zhao, S.; Zhu, C.; Jiang, J. A comparative study of urban expansion in Beijing, Tianjin and Shijiazhuang over the past three decades. *Landsc. Urban Plan.* **2015**, *134*, 93–106. [[CrossRef](#)]
63. The Two-City Green Space Ecological Barrier Project Is Taking Shape. Available online: http://www.tj.gov.cn/sy/zwdt/bmdt/202007/t20200730_3236789.html (accessed on 11 May 2021).